

Logarithmic matching and its applications in computational hydraulics and sediment transport

Accordement logarithmique et applications en hydraulique numérique et en sédimentation

JUNKE GUO, Assistant Professor, Department of Civil Engineering, National University of Singapore, 10 Kent Ridge Crescent, Singapore 119260. E-mail: cveguoj@nus.edu.sg

ABSTRACT

This study presents an asymptotic matching method, the logarithmic matching. It states that for a complicated nonlinear problem or an experimental curve, if one can find two asymptotes, in extreme cases, which can be expressed as logarithmic or power laws, then the logarithmic matching can merge the two asymptotes into a single composite solution. The applications of the logarithmic matching have been successfully tried in several cases in open-channel flows, coastal hydrodynamics and sediment transport such as: 1) the inverse problem of Manning equation in rectangular open-channels, 2) the connection of different laws in computational hydraulics, 3) the solution of linear wave dispersion equation, 4) criterion of wave breaking, 5) wave-current turbulence model, 6) sediment settling velocity, 7) velocity profiles of sediment-laden flows, and 8) sediment transport capacity. All these applications agree very well with numerical solutions or experimental data. Besides, it is pointed out that there are several other cases where the logarithmic matching has potential applications.

RÉSUMÉ

Cette étude présente une méthode d'accordement logarithmique applicable aux problèmes non-linéaires complexes et aux courbes expérimentales. La méthode permet de définir une solution analytique unique composée des fonctions de puissance ou logarithmiques applicables aux asymptotes. Plusieurs applications de la méthode sont présentées pour résoudre des problèmes d'écoulement à surface libre, d'hydrodynamique cotière et de transport de sédiments, tels: 1) problème inverse de l'équation de Manning en canal rectangulaire, 2) application en hydraulique numérique, 3) solution de l'équation de propagation d'onde, 4) critère de déferlement des ondes, 5) écoulements ondulatoires turbulents, 6) vitesse de sédimentation, 7) profils de vitesse d'écoulements chargés de sédiments, et 8) capacité de transport sédimentaire. Toutes ces applications sont en accord avec les solutions analytiques ou avec les données expérimentales. L'article mentionne également d'autres domaines où la méthode d'accordement logarithmique est possiblement applicable.

Keywords: asymptotic matching, logarithmic law, power law, computational hydraulics, sediment transport, linear wave, wave breaking, wave-current turbulence, sediment settling velocity, velocity profiles

1 Introduction

Many complicated natural phenomena, environmental and engineering problems are nonlinear. Many nonlinear problems can be described with logarithmic or power laws (Mandelbrot 1977). For example, a turbulent boundary layer velocity profile can be described with a logarithmic law or a power law (Schlichting 1968; Barenblatt 1996). The widely used Manning equation in open-channel flow is a power law. For capacity-limited sediment transport, the sediment-rating curve often fits a power law of the form: $q_s = aq^b$, in which q_s is unit sediment transport rate, q is unit water discharge, a and b are fitting constants (Julien 1995).

Nonlinear problems are often controlled by several variables. In some cases only certain variables are important while in other cases other variables may dominate problems. Therefore, a nonlinear problem is usually described with two or more logarithmic or power laws. Sediment settling velocity is described by Stokes law, $\omega \propto d^2$, in which ω is settling velocity and d is sediment diameter, for small Reynolds numbers (Chien and Wan, 1999). However, it is described by Newton's law, $\omega \propto d^{1/2}$, for large Reynolds numbers.

Other examples in hydraulic engineering are free flowing and

downstream-influenced weir, flow over a weir and under a gate, drying up of a channel when upstream discharge decreases, resistance laws in alluvial rivers for flat bed and for the case of bed forms, turbulent jets and plumes, etc. It is emphasized that for any numerical simulation, if it involves any of the above problems, continuity (if possible in a derivable way) between two formulas is necessary. Otherwise, unstable numerical oscillations develop systematically in any simulation model and ruin the numerical results (Cunge et al. 1980).

This paper will present an asymptotic matching method, the logarithmic matching, for matching the two asymptotic solutions as a single composite one if the asymptotes can be expressed with logarithmic or power functions. To illustrate its potential applications in computational hydraulics and sediment transport, several nonlinear problems in open-channel flows, coastal hydrodynamics, and sediment transport will be discussed.

2 The logarithmic matching

Suppose one can find the two asymptotic solutions for a nonlinear problem, using an analytical method or experimental method. The two asymptotes can be expressed by or transformed into the fol-

Revision received June 13, 2001. Open for discussion till February 28, 2003.

lowing:

$$y = K_1 \ln x + C_1 \quad (1)$$

for $x \ll x_0$, and

$$y = K_2 \ln x + C_2 \quad (2)$$

for $x \gg x_0$. In the two equations above, x is an independent variable, y is a dependent variable, K_1 and K_2 are two slopes based on a logarithmic scale, shown in Fig. 1, C_1 and C_2 are two intercepts, and x_0 is a reference of x .

To merge the two asymptotes (1) and (2) into a single composite equation, the following two logarithmic models are proposed. Model I is

$$y = K_1 \ln x + \alpha \ln \left[1 + \left(\frac{x}{x_0} \right)^\beta \right] + C_1 \quad (3)$$

and Model II is

$$y = K_2 \ln x - \alpha \ln \left\{ 1 - \exp \left[- \left(\frac{x}{x_0} \right)^\beta \right] \right\} + C_2 \quad (4)$$

In the above two equations α and x_0 are determined with K_1 , K_2 , C_1 and C_2 , and β is a transitional shape parameter that is determined by a collocation method or a least-squares method (Griffiths and Smith 1991).

Consider Model I. It is easy to see that for $x \ll x_0$,

$$\ln \left[1 + \left(\frac{x}{x_0} \right)^\beta \right] \rightarrow 0 \quad (5)$$

then (3) reduces to (1). For $x \gg x_0$, one has

$$\ln \left[1 + \left(\frac{x}{x_0} \right)^\beta \right] \rightarrow \beta \ln x - \beta \ln x_0 \quad (6)$$

Substituting the equation above into (3) gives that

$$y = (K_1 + \alpha\beta) \ln x + (C_1 - \alpha\beta \ln x_0) \quad (7)$$

Comparing (7) with (2) yields

$$K_1 + \alpha\beta = K_2 \quad (8)$$

and

$$C_1 - \alpha\beta \ln x_0 = C_2 \quad (9)$$

The two equations above lead to

$$\alpha = \frac{K_2 - K_1}{\beta} \quad (10)$$

and

$$x_0 = \exp \left(\frac{C_1 - C_2}{K_2 - K_1} \right) \quad (11)$$

Now one can see that x_0 is the cross point of the two asymptotes, shown in Fig. 1. Therefore, Model I can be further written as

$$y = K_1 \ln x + \frac{K_2 - K_1}{\beta} \ln \left\{ 1 + \left(\frac{x}{x_0} \right)^\beta \right\} + C_1 \quad (12)$$

in which x_0 is determined by (11), and β is a transitional shape parameter that is the only undetermined parameter. Note that the logarithmic matching fails when $K_1 = K_2$.

Similarly, one can show that for Model II, (4) can be written as

$$y = K_2 \ln x + \frac{K_1 - K_2}{\beta} \ln \left\{ 1 - \exp \left[- \left(\frac{x}{x_0} \right)^\beta \right] \right\} + C_2 \quad (13)$$

in which x_0 and β are similar to those in (12). Equation (12) or (13) is the solid line in Fig. 1.

Note that (12) and (13) are only two simple ways in many possible connections. In practice, one may compare the two expressions by an error analysis and pick up the better one.

Determination of the value of β

The value of β is an undetermined parameter that can be found by using the collocation method or the least-squares method. Suppose one has a nonlinear problem that is governed by

$$F(x, y) = 0 \quad (14)$$

in which x is independent and y is dependent. Substituting (12) or (13) into (14) gives the corresponding residual R as

$$R(x, \beta) = F(x, f(x, \beta)) \quad (15)$$

in which $f(x, \beta)$ is the expression of (12) or (13) on the right-hand side.

The collocation method gives the value of β by setting the residual $R = 0$ at a certain point such as the cross point $x = x_0$, i.e.,

$$R(x_0, \beta) = 0 \quad (16)$$

The least-squares method is to minimize the squared residual over the solution domain, i.e., find the value of β by solving

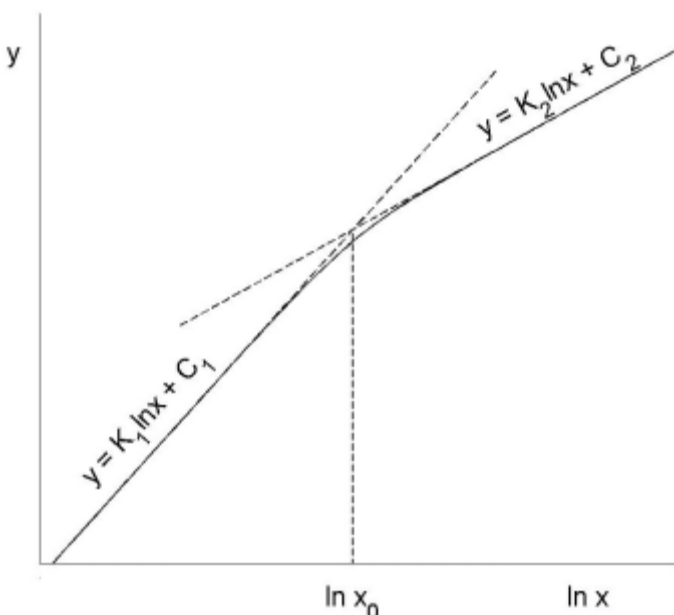


Fig. 1 The scheme of the logarithmic matching

$$\frac{\partial}{\partial \beta} \int_a^b R^2(x, \beta) dx = 0 \quad (17)$$

in which a and b are the lower and the upper limits of the solution domain. The least-squares method (17) usually gives a better result. However, the collocation method (16) is easy to use.

Note that the governing equation (14) can be any type of equations such as differential equations, integral equations or algebraic equations. If a governing equation cannot be formulated, experimental data may be used when determining the value of β .

3 Procedures of applying the logarithmic matching

The following procedures are exercised when one applies the logarithmic matching.

1. Find the two asymptotes by using an analytical method or dimensional analysis method. If the asymptotes are power laws, transform them into logarithmic functions. Note that since the two asymptotes usually result from different mechanisms, they are often expressed with different variables. To apply the logarithmic matching, one must transform the two asymptotes into the same dimensionless independent and dependent variables.
2. With the two asymptotes, like (1) and (2), one can determine the slopes K_1 and K_2 and the intercepts C_1 and C_2 . If $K_1 = K_2$, stop applying the logarithmic matching. Otherwise move to next step.
3. Calculate the cross point x_0 from (11).
4. Construct a general approximate solution by (12) or (13).
5. Substitute (12) or (13) into the governing equation (14) and form a residual function $R(x, \beta)$.
6. Solve the parameter β by applying the collocation method (16) or the least-squares method (17).
7. Finally, see if the single composite solution can be simplified.

4 Applications in open-channel flows

4.1 Inverse problem of Manning equation in rectangular open-channels

Manning equation is usually employed in computation of uniform flows, particularly in channel designs. It is written as

$$V = \frac{\phi}{n} R^{2/3} S^{1/2} \quad (18)$$

or

$$Q = \frac{\phi}{n} \frac{A^{5/3}}{P^{2/3}} S^{1/2} \quad (19)$$

in which V is cross-sectional average velocity, $\phi = 1$ for SI units and 1.49 for English units, n is Manning's coefficient, R is hydraulic radius, S is channel slope, Q is channel discharge, A is cross-sectional area, and P is wetted perimeter. The continuity

equation $Q = AV$ and the definition $R = A/P$ have been used in (19).

For a rectangular channel, one has

$$A = By_n \quad \text{and} \quad P = B + 2y_n \quad (20)$$

in which B is the channel width, and y_n is the normal depth. Substituting (20) into (19) gives that

$$Q = \frac{\phi}{n} \frac{(By_n)^{5/3}}{(B + 2y_n)^{2/3}} S^{1/2} \quad (21)$$

In many cases such as design of a canal and computation of water surface profile, one needs to compute the normal depth y_n for a given discharge Q . This is called the inverse problem of Manning equation. One can see that (21) is nonlinear in terms of y_n . The above equation is usually solved by using design curves, trial-and-error procedures or numerical methods (Chow 1973, French 1994, Chaudhry 1993).

However, applying the logarithmic matching, one can get a simple solution for y_n . Rewrite (21) in dimensionless form, i.e.

$$\frac{nQ}{\phi B^{8/3} S^{1/2}} = \frac{\left(\frac{y_n}{B}\right)^{5/3}}{\left(1 + 2\frac{y_n}{B}\right)^{2/3}} \quad (22)$$

Defining

$$X = \frac{nQ}{\phi B^{8/3} S^{1/2}} \quad \text{and} \quad Y = \frac{y_n}{B} \quad (23)$$

(22) then becomes

$$X = \frac{Y^{5/3}}{(1 + 2Y)^{2/3}} \quad (24)$$

For a wide channel, i.e., $Y \rightarrow 0$, where the resistance due to the side-walls can be neglected, the above equation becomes

$$Y = X^{3/5} \quad (25)$$

or

$$\ln Y = \frac{3}{5} \ln X \quad (26)$$

Defining $x = X$ and $y = \ln Y$, comparing (26) with (1) gives that

$$K_1 = \frac{3}{5} \quad \text{and} \quad C_1 = 0 \quad (27)$$

For a very narrow channel, i.e., $Y \rightarrow \infty$, where the resistance due to the bottom may be neglected, (24) becomes

$$Y = 2^{2/3} X \quad (28)$$

or

$$\ln Y = \ln X + \frac{2}{3} \ln 2 \quad (29)$$

Comparing it with (2) gives

$$K_2 = 1 \quad \text{and} \quad C_2 = \frac{2}{3} \ln 2 \quad (30)$$

With (27) and (30), from (11) one can calculate the cross point at

$$X_0 = \exp\left(\frac{0 - \frac{2}{3} \ln 2}{1 - 3/5}\right) = 2^{-5/3} \quad (31)$$

Choosing Model I, applying (27), (30) and (31) into (12), where $x = X$ and $y = \ln Y$, gives that

$$\ln Y = \frac{3}{5} \ln X - \frac{2}{5\beta} \ln\left[1 + (2^{5/3} X)^\beta\right]$$

or

$$Y = X^{3/5} \left[1 + (2^{5/3} X)^\beta\right]^{2/(5\beta)} \quad (32)$$

The rest is to determine the value of β . From (24) the residual R is defined as

$$R = X - \frac{Y^{5/3}}{(1 + 2Y)^{2/3}} \quad (33)$$

Substituting (32) into the above and setting $R = 0$ at the point $X_0 = 2^{-5/3}$ (the collocation method), one obtains

$$\beta = 0.7824 \quad (34)$$

A comparison between (32) where $\beta = 0.7824$ and a numerical solution is shown in Fig. 2. The maximum relative error is 1.94% that is sufficient in practice. Furthermore, if more accuracy is required, the result from the logarithmic matching may be considered the first approximation. Thus, the convergence will speed up in an iterative technique. A similar procedure may be applied to find the normal depth in trapezoidal channels.

4.2 Potential applications in computational hydraulics

In computational hydraulics, many empirical relations are approximated with power laws. The rating curve of a hydraulic structure,

which is often a boundary condition in a numerical simulation, is often a power function of the upstream water head. The geometric parameters such as the top width, wetted parameter, cross-sectional area, hydraulic radius, and hydraulic depth, of a channel cross-section are often approximated to be power functions of flow depth.

However, the exponents of the power laws of a rating curve may vary with the water surface elevation if the geometry of the hydraulic structure has an abrupt change. When flow passes a gated weir, for a lower water surface elevation, shown in Fig. 3a, the rating curve is characterized by a weir formula (French 1985), i.e.

$$Q = C_w \sqrt{g} B H^{3/2} \quad (35)$$

or

$$\frac{Q}{\sqrt{g} B^{5/2}} = C_w \left(\frac{H}{B}\right)^{3/2} \quad (36)$$

in which Q is the discharge, g is the gravitational acceleration, B is the width of the weir, H is the upstream water head over the top of the weir, and C_w is the weir coefficient.

For a higher water surface elevation, shown in Fig. 3b, the rating curve is characterized by a sluice gate equation (French 1985), i.e.

$$\frac{Q}{\sqrt{g} B^{5/2}} = C_g \left(\frac{d}{B}\right) \left(\frac{H}{B}\right)^{1/2} \quad (37)$$

or

$$\frac{Q}{\sqrt{g} B^{5/2}} = C_g \left(\frac{d}{B}\right) \left(\frac{H}{B}\right)^{1/2} \quad (38)$$

in which C_g is the sluice gate coefficient, and d is the gate opening.

One can see that for a lower upstream water stage, the discharge is proportional to $H^{3/2}$ while for a higher upstream water stage, the discharge is proportional to $H^{1/2}$. The transition between the two laws must be gradual and continuous.

To apply the logarithmic matching, one can assume

$$X = H/B \quad \text{and} \quad Y = Q/(\sqrt{g} B^{5/2}) \quad (39)$$

then according to Model I (12), one has

$$Y = \frac{C_w X^{3/2}}{\left[1 + \left(\frac{X}{X_0}\right)^\beta\right]^{1/\beta}} \quad (40)$$

in which $X_0 = (C_g d)/(C_w B)$, and β is determined by experimental

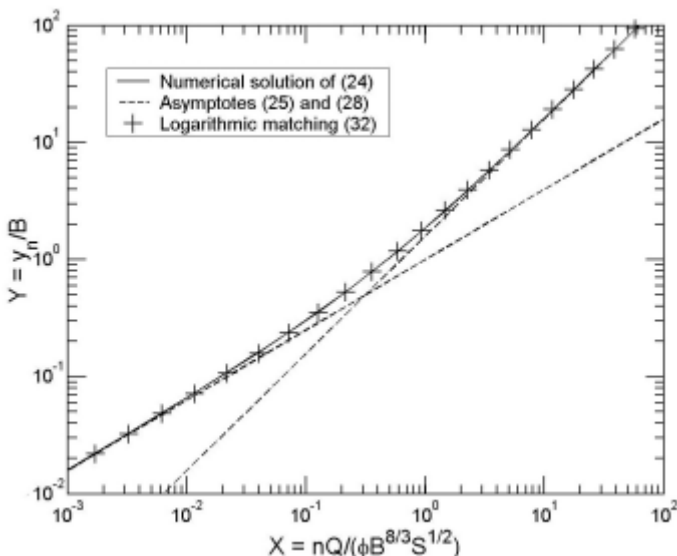


Fig. 2 Comparison of normal depth between a numerical solution and the logarithmic matching solution

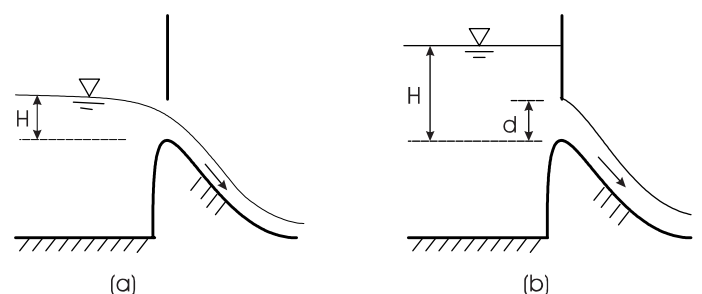


Fig. 3 The scheme of a gated weir

data. In practice, one can first determine the coefficients C_w and C_g according to experimental data, then the value of β is determined at the point $X = X_0$ in the transition zone.

A similar method can also be applied to a rating curve of a hydrological station where if the cross-section comprises a main channel and a flood plain. Another potential application in computational hydraulics is to approximate the variations of geometric parameters such as the top width, wetted perimeter, and cross-sectional area with flow depth in a compound cross-section.

It is emphasized again that the logarithmic matching is significant in practice since if the two different laws, like (35) and (37), are not connected smoothly, its derivative is discontinuous at the transition point. In a finite-difference or finite-element simulation model, if Newton-Raphson iterative method is employed to solve the numerical model, the derivative in the transition zone will be back and forth between the two laws, thus unstable numerical oscillations may develop systematically in any numerical model and ruin the computational results (Cunge et al. 1980).

5 Applications in coastal hydrodynamics

5.1 Solution of wave dispersion equation

Wave length, height, period and flow depth are fundamental parameters for nearly all wave related problems. In practice, wave height, period and flow depth are given by field measurements. The wave length is usually calculated by a dispersion equation, i.e., the relationship among wave length, period and flow depth, which is given by a wave theory. The most popular dispersion equation is given by the linear wave theory (Dean and Dalrymple 1991), i.e.

$$\sigma^2 = gk \tanh kh \quad (41)$$

in which $\sigma = 2\pi/T$ is angular frequency, T is wave period, g is the gravitational acceleration, $k = 2\pi/L$ is wave number, L is wave length, and h is flow depth.

Since (41) is nonlinear with respect to k , one cannot find an analytical solution. Two asymptotes are used in practice, i.e.

$$\sigma^2 = ghk^2 \quad (42)$$

for shallow water $kh \rightarrow 0$, and

$$\sigma^2 = gk \quad (43)$$

for deep water $kh \rightarrow \infty$.

Based on (42) and (43), an approximate general solution for k may be constructed. For simplicity, one can define that

$$X = h\sigma/\sqrt{gh} \quad \text{and} \quad Y = kh \quad (44)$$

Then (41) becomes

$$X^2 = Y \tanh Y \quad (45)$$

(42) and (43) become

$$Y = X \quad (46)$$

for shallow water $Y \rightarrow 0$, and

$$Y = X^2 \quad (47)$$

for deep water $Y \rightarrow \infty$.

Since (41) has a property of exponential function, Model II (13) is then chosen for this case. Transforming (46) and (47) into logarithmic forms and applying the matching II (13), one can get

$$Y = X^2 [1 - \exp(-X^\beta)]^{-1/\beta} \quad (48)$$

where in the derivation, $K_1 = 1$, $C_1 = 0$, $K_2 = 2$, $C_2 = 0$ and $X_0 = 1$. The residual in this case is defined according to (45), i.e.

$$R = X^2 - Y \tanh Y \quad (49)$$

Substituting (48) into the above equation gives that

$$R = X^2 - X^2 [1 - \exp(-X^\beta)]^{-1/\beta} \tanh \left\{ X^2 [1 - \exp(-X^\beta)]^{-1/\beta} \right\} \quad (50)$$

The collocation method at $X_0 = 1$ gives

$$R|_{X=1} = 1 - (1 - e^{-1})^{-1/\beta} \tanh \left[(1 - e^{-1})^{-1/\beta} \right] = 0 \quad (51)$$

which yields that

$$\beta = 2.5194 \quad (52)$$

Using the least-squares method, the parameter β is found by solving

$$\frac{\partial}{\partial \beta} \int_0^\infty R^2 = 0 \quad (53)$$

A numerical estimation of (50) and (53) using a MatLab function gives that

$$\beta = 2.4908 \quad (54)$$

One can see that the two methods give very similar results. Fig. 4 shows an excellent agreement between (48) where $\beta = 2.4908$ and a numerical solution. An error analysis shows that (48) with $\beta = 2.4908$ has an accuracy of 0.75% over $0 \leq X \leq \infty$.

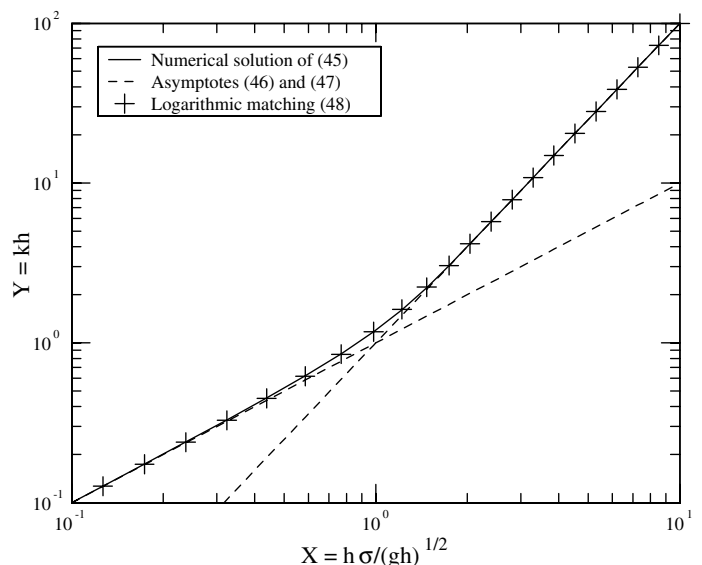


Fig. 4 Comparison of wave number between a numerical solution and the logarithmic matching solution

With wave number k available from (48) and (54), one can calculate the corresponding wave length L and celerity c by

$$L = \frac{2\pi}{k} \quad \text{and} \quad c = \frac{L}{T} \quad (55)$$

Furthermore, other wave parameters (Kamphuis 2000, p33-34) for any water depth can be obtained.

5.2 Criterion of wave breaking

The criterion of wave breaking is another important parameter in coastal hydrodynamics and sediment transport. A general theoretical criterion for wave breaking is still inadequate because of the complex. However, in shallow water with a mild beach, the solitary wave theory criterion (Dean and Dalrymple 1991, Kamphuis 2000) is quite good, i.e.

$$\frac{H_b}{h} = 0.78 \quad (56)$$

in which H_b is the wave height at breaking point, and h is the corresponding water depth.

For deep water, Miche criterion (Kamphuis 2000) that is based on the Stokes wave solution is valid, i.e.

$$\frac{H_b}{L_0} = 0.142 \quad (57)$$

where

$$L_0 = 1.2 \left(\frac{gT^2}{2\pi} \right) \quad (58)$$

is the wave length in deep water that includes nonlinear effects. In (58) g is the gravitational acceleration, and T is the wave period. Substituting (58) into (57) gives that

$$\frac{H_b}{gT^2} = 0.027 \quad (59)$$

One can rewrite (56) in the format of (59), i.e.

$$\frac{H_b}{gT^2} = 0.78 \left(\frac{h}{gT^2} \right) \quad (60)$$

Defining $X = h/(gT^2)$ and $Y = H_b/(gT^2)$, (60) and (59) become

$$Y = 0.78X \quad (61)$$

for shallow water, and

$$Y = 0.027 \quad (62)$$

for deep water. Equations (61) and (62) and some observed data are plotted in Fig. 5. One can see that the transition from shallow water to deep water is gradual. Therefore, the logarithmic matching can be applied to find the criterion in the transition.

Applying the logarithmic matching I (12) to (61) and (62), one can show that the general wave breaking criterion is

$$Y = \frac{0.78X}{\left[1 + \left(\frac{X}{X_0} \right)^\beta \right]^{1/\beta}} \quad (63)$$

in which $X_0 = 0.0346$ and $\beta = 2$. The value of β is determined by the collocation method at $X_0 = 0.0346$ where the corresponding

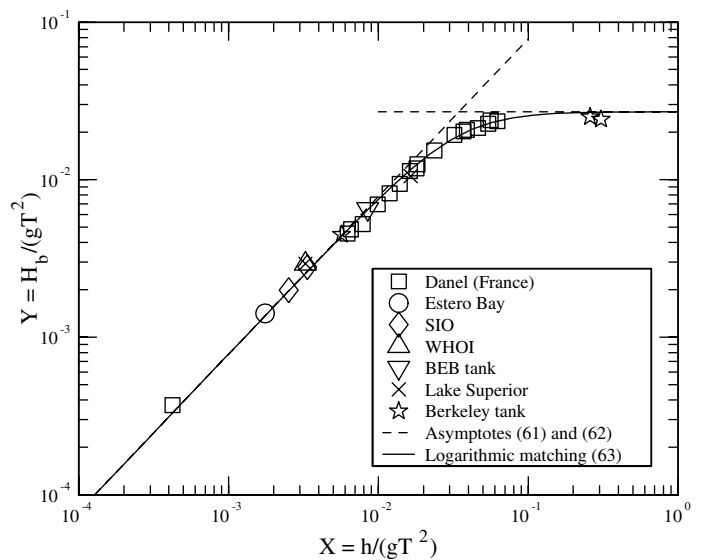


Fig. 5 Breaking criterion for mild beaches and deep water (Data source: Dean and Dalrymple, 1991, p336)

observed value is $Y = 0.191$. The average relative error of (63) is 5.3%. A similar criterion can also be established by Model II (13).

5.3 Wave-current turbulence model

Wave-current interaction is very complicated. This paper does not go to the physics of the wave-current model. It will only show that the logarithmic matching may be a way to improve the existing eddy viscosity model. The G-M model, proposed by Grant and Madsen (1979), is the simplest and a classical model in wave-current turbulence. It claims that the wave-current turbulent boundary layer essentially consists of two sublayers, i.e., a wave boundary layer and a current boundary layer.

Near the bed, because of the superposition of a wave boundary and a current boundary, turbulence becomes stronger in wave-current boundary than in a pure current boundary. The classical eddy viscosity model is still valid except that the shear velocity is characterized by its maximum value, i.e.

$$\nu_t = \kappa u_{*m} z \quad (64)$$

in which ν_t is eddy viscosity, $\kappa = 0.4$ is von Karman constant, $u_{*m} = \sqrt{u_{*wm}^2 + u_{*c}^2}$ is the maximum shear velocity due to both the maximum wave shear velocity u_{*wm} and the current shear velocity u_{*c} , and z is the distance from the bed.

The eddy viscosity model (64) results in the following logarithmic law,

$$u_c = \frac{u_{*c}}{\kappa} \frac{u_{*c}}{u_{*m}} \ln \frac{z}{z_0} \quad (65)$$

in which u_c is the current velocity at a distance z from the bed, and z_0 is the hydraulic roughness of the bed that is equal to $k_s/30$ in which k_s is Nikuradse roughness.

If one defines a wave boundary layer thickness δ_{wc} , the above equation can be rearranged as

$$\frac{u_c}{u_{*c}} = \frac{1}{\kappa} \frac{u_{*c}}{u_{*m}} \ln \frac{z}{\delta_{wc}} - \frac{1}{\kappa} \frac{u_{*c}}{u_{*m}} \ln \frac{z_0}{\delta_{wc}} \quad (66)$$

Equations (64)-(66) are only valid in the waver boundary layer, i.e., $z < \delta_{wc}$.

The wave boundary layer is usually so thin that it does not affect the current flow in the main flow region. Thus, the eddy viscosity is the same as that in a pure current boundary layer, i.e.

$$v_t = \kappa u_{*c} z \quad (67)$$

the resultant current velocity profile is then independent of the wave boundary except that the hydraulic roughness increases, i.e.

$$u_c = \frac{u_{*c}}{\kappa} \ln \frac{z}{z_{0a}} \quad (68)$$

in which z_{0a} is the apparent hydraulic roughness that includes the effect of the wave boundary layer.

The above equation can alternatively be written as

$$\frac{u_c}{u_{*c}} = \frac{1}{\kappa} \ln \frac{z}{\delta_{wc}} - \frac{1}{\kappa} \frac{u_{*c}}{u_{*m}} \ln \frac{z_{0a}}{\delta_{wc}} \quad (69)$$

The above two equations are valid for $z = \delta_{wc}$.

Based on (66) and (69), a composite law may be established according to (12), i.e.

$$\frac{u_c}{u_{*c}} = \frac{1}{\kappa} \frac{u_{*c}}{u_{*m}} \ln \frac{z}{z_0} + \frac{1}{\beta \kappa} \left(1 - \frac{u_{*c}}{u_{*m}} \right) \ln \left[1 + \left(\frac{z_0}{\delta_{wc}} \right)^\beta \right] \quad (70)$$

in which β is the transitional parameter that may vary with the relative wave intensity u_{*m}/u_{*c} and the angle between the wave and the current directions. All parameters except β are estimated by Madsen's method (Madsen and Grant 1976, Mathisen and Madsen 1996). Fig. 6 is a comparison of (70) with one of Mathisen and Madsen's (1996) flume experiments (Expt B) where $u_{*c} = 3.15$ cm/s, $u_{*wm} = 6.36$ cm/s, $u_{*m} = 7.10$ cm/s, $z_0 = 0.6$ cm and $\delta_{wc} = 6$ cm. The value of β is fitted to be 10 in

this case. It shows that the structure of (70) is correct. Note that a velocity $u_w = -1.8$ cm/s, due to nonlinear wave mass transport, has been accounted for in Fig. 6. A further explanation about the wave-induced mass transport is referred to Mathisen and Madsen (1996).

Furthermore, an eddy viscosity equation may be deduced from (70) that can smoothly connect the two sublayers. The new eddy viscosity equation may be helpful in the study of sediment concentration distribution.

6 Applications in sediment transport

6.1 Sediment settling velocity

Sediment settling velocity is a very basic parameter in sediment transport. It figures prominently in all sediment transport problems. Many empirical equations have been proposed by different investigators. The summary of those equations can be found in several textbooks or manuals (Graf 1971, Yalin 1977, Raudkivi 1990, Chien and Wan 1999, and others). In view of practice, this subject has been well studied. However, one will see that a very simple formula for sediment settling velocity can be derived by applying the logarithmic matching.

It is well-known that for a small Reynolds number $Re = \omega d/\nu < 1$ where ω is sediment settling velocity, d is sediment diameter, and ν is fluid kinematic viscosity, the sediment settling velocity has a theoretical solution, i.e., Stokes equation,

$$\omega = \frac{1}{24} \frac{(s-1)gd^2}{\nu} \quad (71)$$

in which $s = \rho_s/\rho$ is sediment specific weight, ρ_s is sediment density, ρ is fluid density, and g is the gravitational acceleration. Note that the above equation is for natural sands. For a sphere the constant is 18 instead of 24.

When Reynolds number is very large, i.e., $Re = \omega d/\nu > 10^3$, the settling velocity is expressed by Newton's law, i.e.

$$\omega = \sqrt{\frac{4}{3C_D}(s-1)gd} \quad (72)$$

in which $C_D \approx 1$ according to experimental data (Sha 1965). The above equation is then further written as

$$\omega = \sqrt{\frac{4}{3}(s-1)gd} \quad (73)$$

Obviously, if one defines a dimensionless sediment diameter, i.e.

$$d_* = \left[\frac{(s-1)gd^3}{\nu^2} \right]^{1/3} \quad (74)$$

then (71) and (73) become

$$Re = \frac{d_*^3}{24} \quad (75)$$

for $Re < 1$, and

$$Re = \left(\frac{4}{3} \right)^{1/2} d_*^{3/2} \quad (76)$$

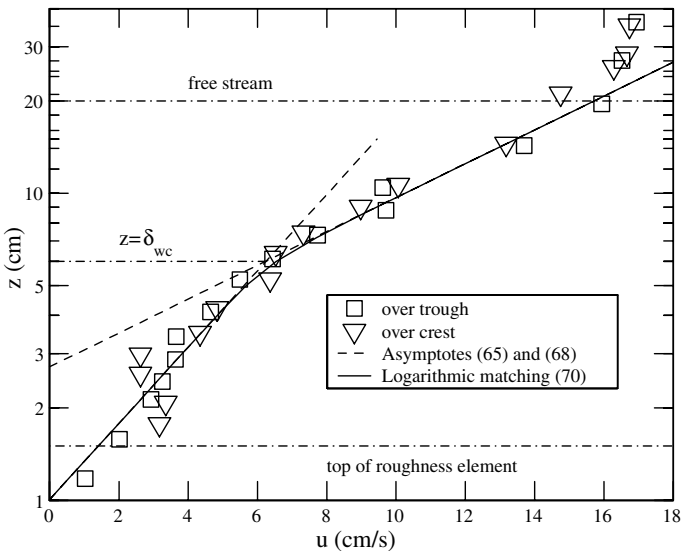


Fig. 6 Comparison of equation (70) with Mathisen and Madsen's (1996) experimental data (Expt B) of wave-current flow

for $Re > 10^3$.

Transforming (75) and (76) into logarithmic forms, one then has

$$K_1 = 3, \quad C_1 = -\ln 24 \quad (77)$$

and

$$K_2 = \frac{3}{2}, \quad C_2 = \frac{1}{2} \ln\left(\frac{4}{3}\right) \quad (78)$$

The cross point is then calculated from (11), i.e.

$$d_{*0} = 24^{2/3} \left(\frac{4}{3}\right)^{1/3} = 768^{1/3} \quad (79)$$

Choosing Model I, from (12) one has

$$\ln Re = 3 \ln d_* - \frac{3}{2\beta} \ln \left[1 + \left(\frac{d_*}{768^{1/3}} \right)^\beta \right] - \ln 24$$

or

$$Re = \frac{d_*^3}{24} \left[1 + \left(\frac{d_*}{768^{1/3}} \right)^\beta \right]^{-\frac{3}{2\beta}} \quad (80)$$

According to the experimental data in Fig. 7, $Re \approx 16$ at $d_* = 768^{1/3}$. This leads to the value of $\beta \approx 1.5$. Thus, (80) becomes

$$Re = \frac{d_*^3}{24 + \frac{\sqrt{3}}{2} d_*^{3/2}} \quad (81)$$

This equation can be considered a general formula for sediment settling velocity. Its comparison with observed data is shown in Fig. 7. The average value of the relative errors is 5.69%.

One can show that the above equation can be alternatively written as

$$\frac{\omega}{\sqrt{(s-1)gd}} = \left(\frac{6}{S_*} + \frac{\sqrt{3}}{2} \right)^{-1} \quad (82)$$

if one defines

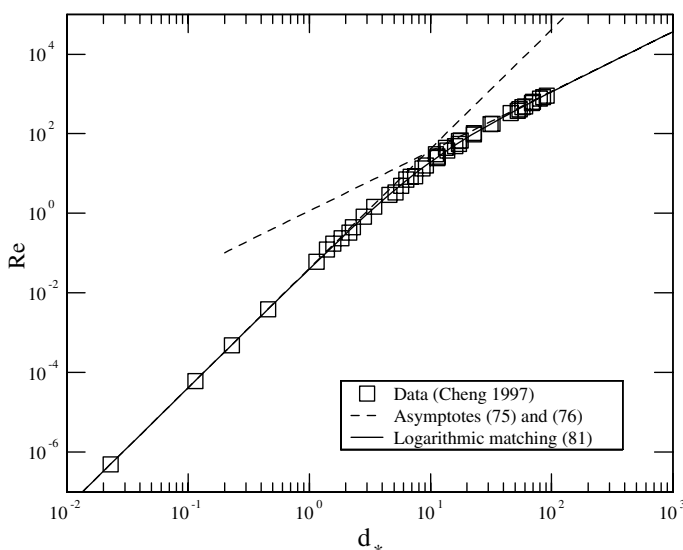


Fig. 7 Comparison of equation (81) with experimental data

$$d_*^3 = \frac{(s-1)gd^3}{v^2} = 16S_*^2$$

and

$$Re = \frac{\omega d}{v} = 4S_* \cdot \frac{\omega}{\sqrt{(s-1)gd}}$$

in which $S_* = d\sqrt{(s-1)\rho}/(4\mu)$ is the sediment-fluid parameter introduced by Madsen and Grant (1976).

Equation (82) is similar to Madsen's (Guo 2000) empirical formula, i.e.

$$\frac{\omega}{\sqrt{(s-1)gd}} = \left(\frac{5.4}{S_*} + 0.9 \right)^{-1} \quad (83)$$

The slight differences of the constants might result from different data sources.

It is noteworthy that in some cases, one may need to know the drag coefficient C_D which can be found from (72), i.e.

$$C_D = \frac{4}{3} \left(\frac{\omega}{\sqrt{(s-1)gd}} \right)^{-2} \quad (84)$$

Unlike (72), this equation is valid for any Reynolds number. Substituting (82) into (84) gives

$$C_D = \frac{4}{3} \left(\frac{6}{S_*} + \frac{\sqrt{3}}{2} \right)^2 \quad (85)$$

which shows that one can calculate the drag coefficient C_D without sediment settling velocity ω .

Similar procedures can be applied to the settling velocity of spheres. The results are

$$Re = \frac{d_*^3}{18 + \frac{d_*^{3/2}}{\sqrt{3}}} \quad (86)$$

or

$$\frac{\omega}{\sqrt{(s-1)gd}} = \left(\frac{4.5}{S_*} + \frac{1}{\sqrt{3}} \right)^{-1} \quad (87)$$

and

$$C_D = \frac{4}{3} \left(\frac{4.5}{S_*} + \frac{1}{\sqrt{3}} \right)^2 \quad (88)$$

By the way, Cheng's (1997) formula can be derived by applying the logarithmic matching to the drag coefficient with $\beta = 1.5$.

6.2 Effect of sediment suspension on turbulent velocity profiles

Vanoni (1946), Einstein and Chien (1955), and Elata and Ippen (1971) experimentally showed that the logarithmic velocity profile is still valid in the main flow region of sediment-laden flows except that the von Karman constant κ decreases with sediment suspension. Later Coleman (1986) and others claimed that sediment suspension does not affect the velocity profile near the bed. In other words, the von Karman constant κ is the same in sedi-

ment-laden flow as in a clear water flow near the bed. Thus, the velocity profile in a sediment-laden flow can be described with two logarithmic laws.

Near the bed, following to Coleman (1986), the velocity profile can be expressed by

$$\frac{u}{u_*} = \frac{1}{\kappa} \ln \xi + C_1 \quad (89)$$

in which u is the velocity at a distance ξ from the bed, ξ is normalized by the flow depth, u_* is shear velocity, C_1 is an integration constant, and $\kappa = 0.4$ is the von Karman constant in clear water.

In the main flow region, following Vanoni (1946) and others, the velocity profile may be expressed with

$$\frac{u}{u_*} = \frac{1}{\kappa_m} \ln \xi + C_2 \quad (90)$$

in which κ_m is the von Karman constant in the main flow region which is less than 0.4 and varies with sediment suspension, and C_2 is another integration constant.

Putting aside the physical mechanism and emphasizing the analysis technique in this paper, one may write the above two equations as a composite velocity profile, i.e.

$$\frac{u}{u_*} = \left(\frac{1}{\kappa} \ln \xi + C_1 \right) + \frac{1}{\beta} \left(\frac{1}{\kappa_m} - \frac{1}{\kappa} \right) \ln \left[1 + \left(\frac{\xi}{\xi_0} \right)^\beta \right] \quad (91)$$

in which ξ_0 can be found from (11), i.e.

$$\xi_0 = \exp \left(\frac{C_1 - C_2}{\frac{1}{\kappa_m} - \frac{1}{\kappa}} \right) \quad (92)$$

and β is a transition parameter. Fig. 8 shows a comparison between (91) and Einstein and Chien's (1955) flume data (S-15) where $\kappa = 0.4$, $C_1 = 17$, $\kappa_m = 0.168$, $C_2 = 26.25$ and $\beta = 4$. A sys-

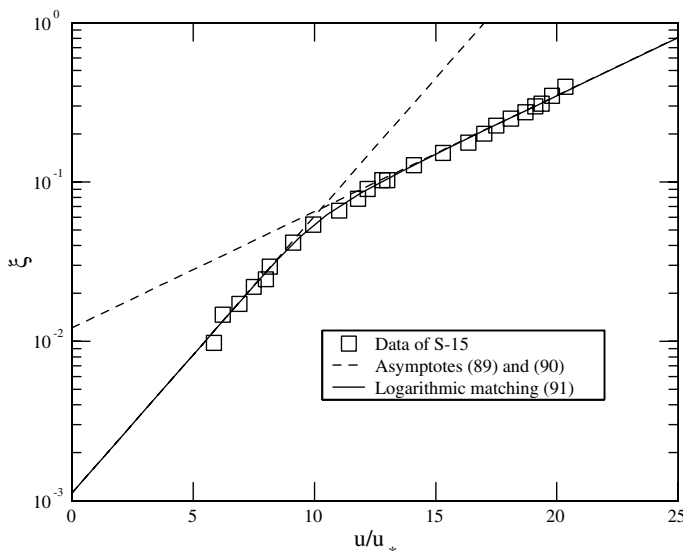


Fig. 8 Comparison of the velocity profile (91) with Einstein and Chien's (1955) experiments (S-15)

tematic analysis, including its physical mechanism and parameter variations with sediment suspension, may be reported separately in the future.

Note that the second term in (91) can be considered a wake function in sediment-laden flows.

6.3 Sediment transport capacity

Most sediment transport capacity formulas have power forms (Julien 1995). Based on an analysis of turbulent kinetic energy, Zhang Ruijin (Zhang and Xie 1993) proposed the following semi-empirical equation:

$$S_* = K \left(\frac{U^3}{gR\omega} \right)^m \quad (93)$$

in which S_* is transport capacity in terms of kg/m^3 , U is cross-sectional average velocity, g is the gravitational acceleration, R is hydraulic radius, ω is sediment settling velocity. The dimensionless factor $U^3/(gR\omega)$ expresses the relative strength of turbulent diffusivity to sediment gravity. K and m are model parameters and K has the same unit as S_* .

Zhang's equation has been widely used in the Yellow River, the Yangtze River, and other China rivers. Its disadvantage is that both K and m are not constant and vary with $U^3/(gR\omega)$, shown in Fig.9. This makes (93) inconvenient in practice.

However, based on the observed data in Fig. 9, one has the lower asymptote,

$$S_* = \frac{1}{20} \left(\frac{U^3}{gR\omega} \right)^{1.5} \quad (94)$$

for $U^3/(gR\omega) < 10$, and the upper asymptote,

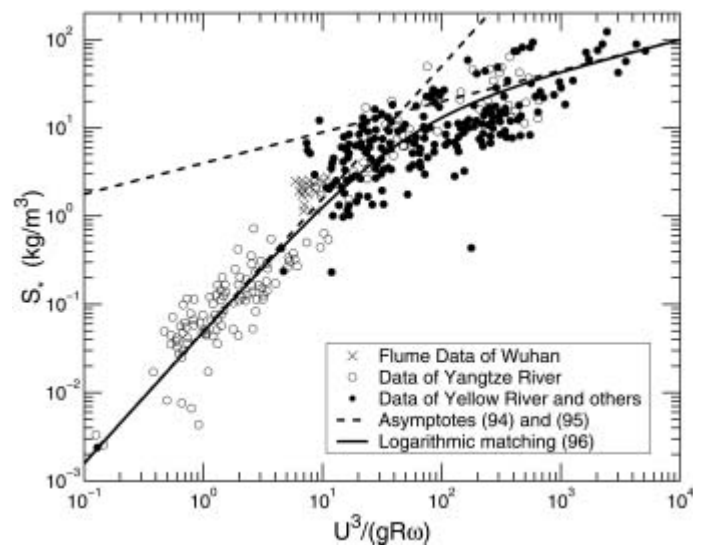


Fig. 9 Comparison of the improved Zhang's sediment transport capacity equation (96) with flume and field data (Data source: Zhang and Xie 1993, p58)

$$S_* = 3.98 \left(\frac{U^3}{gR\omega} \right)^{0.35} \quad (95)$$

for $U^3/(gR\omega) > 10^3$. According to the matching model (12), one can write a general equation like

$$S_* = \frac{\frac{1}{20} \left(\frac{U^3}{gR\omega} \right)^{1.5}}{1 + \left(\frac{1}{45} \frac{U^3}{gR\omega} \right)^{1.15}} \quad (96)$$

In the derivation, $K_1 = 1.5$, $C_1 = -1n20$, $K_2 = 0.35$, $C_2 = 1n3.98$ and $\beta = 1.15$. Equation (96) is the solid line in Fig. 9 which shows that (96) represents the measured data quite well and is easy to use in practice.

Note that the logarithmic matching may also be applied to improve other transport capacity equations such as Ackers and White's (1973), Zhang's (1992), and Molinas and Wu's (2001). Molinas and Wu (2001) have shown that sediment transport capacity equation follows different power laws of unit stream power for shallow and deep flows. A general transport equation for both shallow and deep flows may be established by applying the logarithmic matching.

7 Other potential applications

Except the above, there are several other cases where the logarithmic matching may be applied. 1) In a turbulent boundary layer flow, the velocity profile obeys the logarithmic law near the wall while it tends to a constant velocity away from the wall. The constant velocity may be considered a special case of a logarithmic law where the slope in terms of a logarithmic scale is zero. 2) In a turbulent hyperconcentrated sediment-laden flow or a debris flow, due to the yield shear stress, a constant velocity zone exists near the water surface. The whole velocity profile is similar to that in a turbulent boundary layer flow. 3) In a non-Newtonian flow or a hyperconcentrated flow, the constitutive equation such as Bagnold's dispersive stresses is usually described by two power laws (Fredsoe and Deigaard 1992). The logarithmic matching may be applied to give a general equation in a numeral simulation. 4) In turbulent jets and plumes, many relations result from a scaling analysis and expressed by two power laws (Fischer, et al., 1979). The results may be improved by applying the logarithmic matching. 5) Green-Ampt method is an implicit method in the estimation of infiltration (Chow et al. 1988). Two power laws of its asymptotes exist so that an explicit solution for infiltration may be established by using the logarithmic matching.

8 Conclusions

For a complicated nonlinear problem, if one can find two asymptotic solutions which are logarithmic functions or can be transformed into logarithmic functions, like equations (1) and (2), then the logarithmic matching (12) or (13) can merge the two asymptotes as a single composite solution. The logarithmic matching involves one undetermined parameter β that expresses the transi-

tional shape between the two asymptotes. The value of β can be determined using a collocation method at the transition point or a least-squares method.

Applications of the logarithmic matching have been successfully tried in several cases in open-channel flows, coastal hydrodynamics and sediment transport. 1) Applying the logarithmic matching, an explicit solution for the inverse problem of Manning equation in rectangular open-channels is derived. 2) Take the discharge laws of a gated weir for an example, it is shown that the logarithmic matching can be used to connect two different discharge laws smoothly in a derivable way. It is further pointed out that the logarithmic matching may be used to improve a numerical algorithm when two different laws must be connected smoothly. Otherwise, numerical oscillations will occur in any simulation model and ruin the computational results. 3) An explicit solution of the linear wave dispersion equation is obtained by applying the logarithmic matching. This solution may save much computational time in a large coastal or ocean numerical simulation. 4) A general criterion of wave breaking in a mild beach has been proposed based on the solitary wave theory, Stokes wave solution and the logarithmic matching. 5) It is shown that the classical wave-current model, the G-M model, may be improved if the logarithmic matching is applied. 6) Two simple equations for sediment settling velocity are derived by applying the logarithmic matching to Stokes law and Newton law. The result agrees well with experimental data. 7) Take one of Einstein and Chien's (1955) experimental data for an example, it is shown that the logarithmic matching may be applied to study the effect of sediment suspension on turbulent velocity profiles. 8) It is shown that Zhang's (Zhang and Xie 1993) sediment transport capacity equation may be greatly improved by applying the logarithmic matching. 9) Finally, several other cases are pointed out where the logarithmic matching has potential applications.

9 Acknowledgements

Prof. Ole S. Madsen of MIT provided useful comments on the first manuscript. Prof. Pierre. Y. Julien of Colorado State University reviewed the final version and translated the title and abstract into French. The comments of the two anonymous reviewers and Associate Editor Prof. J. A. Cunge greatly improved the final version.

10 References

- ACKERS, P. and WHITE, W. R. (1973). Sediment transport: new approach and analysis. *J. Hydr. Div., ASCE*, 99(11), 2041-60.
- BARENBLATT, G. I. (1996). *Scaling, self-similarity, and intermediate asymptotics*. Cambridge University Press.
- CHAUDHRY, M. H. (1993). *Open-Channel Flow*, Prentice-Hall, 87-90.
- CHENG, N. S. (1997). Simplified settling velocity formula for sediment particle. *J. Hydr. Engrg, ASCE*, 123, No. 2, 149-152.
- CHIEN, N. and WAN, Z. H. (1999). *Mechanics of Sediment Transport*, ASCE Press.
- CHOW, V. T. (1973). *Open-Channel Hydraulics*. McGraw-Hill.

- CHOW, V. T., MAIDMENT, D. R. and MAYS, L. W. (1988). *Applied Hydrology*. McGraw-Hill, 116-122.
- COLEMAN, N. L. (1986). Effects of suspended sediment on the open-channel distribution. *Water Resources Research*, AGU, 22, No. 10, 1377-1384.
- CUNGE, J. A., HOLLY, F. M. and VERWEY, A. (1980). *Practical Aspects of Computational River Hydraulics*. Pitman Advanced Publishing Program, Boston.
- DEAN, R. G. and DALRYMPLE, R. A. (1991). *Water Wave Mechanics for Engineers and Scientists*. World Scientific, Singapore.
- EINSTEIN, H. A. and CHIEN, N. (1955). Effects of heavy sediment concentration near the bed on velocity and sediment distribution. U. S. Army Corps of Engineers, Missouri River Division Rep. No. 8.
- ELATA, C. and IPPEN, A. T. (1961). The dynamics of open channel flow with suspensions of neutrally buoyant particles. Technical Report No. 45, Hydrodynamics Lab, MIT.
- FISCHER, H. B., LIST, E. J., KOH, R. C. Y., IMBERGER, J. and BROOKS, N. H. (1979). *Mixing in Inland and Coastal Waters*. Academic Press.
- FREDSOE, J. and DEIGAARD, R. (1992). *Mechanics of Coastal Sediment Transport*. World Scientific, Singapore.
- FRENCH, R. H. (1985). *Open-Channel Hydraulics*. McGraw-Hill.
- GRAF, W. H. (1971). *Hydraulics of Sediment Transport*. McGraw-Hill.
- GRANT, W. D. and MADSEN, O. S. (1979). Combined wave and current interaction with a rough bottom. *J. Geophys. Res.*, 84, 1808.
- GRIFFITHS, D.V. AND SMITH, I.M. (1991). *Numerical Methods for Engineers*. CRC Press, 264-266.
- GUO, J. (2000). Generic logarithmic model and its applications in sediment transport. Proc. 12th Congress of APD-IAHR, Vol. 1, 151-159, Asian Institute of Technology, Bangkok.
- JULIEN, P. Y. (1995). *Erosion and Sedimentation*, Cambridge University Press.
- KAMPHUIS, J. W. (2000). *Introduction to Coastal Engineering and Management*. World Scientific, Singapore.
- MADSEN, O. S. and GRANT, W. D. (1976). Quantitative description of sediment transport by waves. Proc. 15th ICCE, ASCE, 2, 1093-1112.
- MANDELBROT, B. B. (1977). *The Fractal Geometry of Nature*. W. H. Freeman and Company, New York.
- MATHISEN, P. P. and MADSEN, O. S. (1996). Waves and current over a fixed ripple bed, 2. Bottom and apparent roughness experienced by currents in the presence of waves. *J. Geophys. Res.*, 101(C7), 16543-50.
- MOLINAS, A. and WU, B. (2001). Transport of sediment in large sand-bed rivers. *J. Hydr. Res.*, IAHR, 39(2), 135-146.
- RAUDKIVI, A. J. (1990). *Loose Boundary Hydraulics*. 3rd Ed., Pergamon Press.
- SCHLICHTING, H. (1968). *Boundary-Layer Theory*. McGraw-Hill, New York.
- SHA, Y. Q. (1965). *Introduction to Sediment Transport Mechanics*, Industry Press, Beijing, China (in Chinese).
- VANONI, V. A. (1946). Transportation of suspended sediment by running water. *Trans.*, ASCE, 111, 67-133.
- YALIN, M. S. (1977). *Mechanics of Sediment Transport*. 2nd Ed., Pergamon Press.
- ZHANG, H. W. and ZHANG, Q. (1992). Sediment transport capacity equation for the Yellow River, People's Yellow River, No. 11, Zhengzhou, China (in Chinese).
- ZHANG, R. and XIE, J. (1993). *Sedimentation Research in China*. China Water and Power Press, Beijing.

